Theoretical Study on Frenkel Excitons in Mott-Jahn-Teller Insulator A_4C_{60}

Shugo SUZUKI, Jin HIROSAWA, and Kenji NAKAO

Institute of Materials Science, University of Tsukuba, Tsukuba 305-8573

(Received June 15, 2006)

We study low-energy excitations in the Mott-Jahn-Teller insulator A_4C_{60} theoretically, where A is alkali metal. A model which takes account of both the electron-electron and electron-phonon interactions is employed and the low-energy excitations are calculated by using the Tamm-Dancoff approximation. It is found that the lowest excitation corresponds to the creation of the spin-singlet Frenkel excitons at about 0.3 eV and the next lowest excitation corresponds to the creation of the spin-triplet Frenkel excitons at about 0.6 eV. It is also found that the excitations of a pair of a free electron and a free hole lie over 0.8 eV. A remarkable point is that the spin-singlet Frenkel excitons are lower in energy than the spin-triplet Frenkel excitons in A_4C_{60} in contrast to usual insulators.

KEYWORDS: alkali-metal-doped C_{60}, Mott-Jahn-Teller insulator, electron-electron interaction, electron correlation, electron-phonon interaction, Jahn-Teller effect

1. Introduction

In the last decade, the electronic structures of alkali-metal-doped C_{60}, A_xC_{60} where A is alkali metal and x is the valence of C_{60} molecules, have been studied extensively.[1–4] In particular, the superconductivity with relatively high critical temperatures in A_3C_{60} has stimulated a number of studies not only of A_3C_{60} but also of other A_xC_{60}. As a result, a variety of unusual phenomena have been discovered. For instance, it has been shown that the introduction of NH_3 molecules into A_3C_{60} results in the disappearance of superconductivity and the appearance of antiferromagnetic order.[5] Among such anomalies, the most remarkable one is that A_2C_{60} and A_4C_{60} are insulators in contradiction to the prediction of the rigid-band picture.[6–11] Due to the nature of their insulating ground states, these materials are called Mott-Jahn-Teller insulators.[12]

Since the conduction bands of A_xC_{60} are threefold, it is, at first sight, expected that A_xC_{60} is metallic for any x of $0 < x < 6$. Nevertheless, a number of experimental studies have revealed that A_2C_{60} and A_4C_{60} are nonmagnetic insulators.[6–11] Photoemission studies have shown that there is no emission at the Fermi level in the photoemission spectra of A_4C_{60} and also infrared-refraction measurements have shown that there is no Drude-like behaviors in the optical-conductivity spectra of A_4C_{60}.[10] Furthermore, magnetic susceptibility measurements have shown that A_2C_{60} and A_4C_{60} are not only insulating but also nonmagnetic.[6–8] These anomalous behaviors have stimulated several theoretical studies that intended to ex-

plain both the superconductivity in A_3C_{60} and the anomalies in A_2C_{60} nd A_4C_{60} on the same footing.[13–16)]

The key to understand the electronic structures of A_xC_{60} is the electron-electron and electron-phonon interactions.[14–16)] In particular, the threefold degeneracy of the lowest unoccupied molecular orbitals, the t_{1u} level, is of great importance because it results in the Jahn-Teller effect in the C_{60} molecule. In our previous studies, we have proposed that the competition between the electron-electron and electron-phonon interactions is essential to A_3C_{60} while the cooperation between the two interactions is essential to A_2C_{60} and A_4C_{60}.[14–16)] In A_3C_{60}, the electron-electron interaction, i.e., the Coulomb repulsion, prefers a C_{60}^{3-} molecule, assisting uniform charge distribution, while the electron-phonon interaction prefers a C_{60}^{2-} or C_{60}^{4-} molecule due to the Jahn-Teller effect, enhancing charge disproportionation; this competition results in A_3C_{60} to remain metallic despite that both interactions are considerably strong. In A_2C_{60} and A_4C_{60}, on the other hand, both interactions prefer uniform charge distribution where all C_{60} molecules have the equal number of the t_{1u} electrons because such a state is energetically stable not only for the Coulomb repulsion but also for the Jahn-Teller effect. That is, the energy gaps in A_2C_{60} and A_4C_{60} mainly consist of two contributions; one is from the electron-electron interaction and the other is from the electron-phonon interaction.

Although the insulating ground states of A_2C_{60} and A_4C_{60} are successfully explained by considering the electron-electron and electron-phonon interactions simultaneously, it is next necessary to study the excited states of these insulators. Since these two interactions largely contributes to the energy gaps of A_2C_{60} and A_4C_{60}, low-energy excitations in these insulators possibly show remarkable characteristics. For instance, there exist spin-wave excitations in the Mott-Hubbard insulators, which are the collective excitations originated in the antiferromagnetic ground state with the energy gap opened by the electron-electron interaction. It is thus of great interest to study low-energy excitations in A_2C_{60} and A_4C_{60} because the energy gaps are opened by both the electron-electron and electron-phonon interactions.

The purpose of the present paper is to study low-energy excitations in A_4C_{60}. We employ a model used in our previous studies; the electron-electron and electron-phonon interactions are both taken into account in this model. To calculate low-energy excitations in A_4C_{60}, we use the Tamm-Dancoff approximation (TDA) on the basis of insulating ground state of the material obtained by the Hartree-Fock calculation. In §2, the model is briefly explained. In §3, we derive the equation of motion of the operators which create excitations within the TDA. The results and discussion are given in §4. Finally, we summarize the present study in §5.

2. Model

In this section, we briefly explain our model previously employed to study the properties of A_xC_{60}.[14–16)] In the present study, we consider a model which takes account of both the electron-electron and electron-phonon interactions within the antiadiabatic approximation.

In this approximation, the phonon frequencies are assumed to be sufficiently larger than the width of the t_{1u} bands. The effective Hamiltonian within the antiadiabatic approximation is obtained by eliminating the phonon degree of freedom. The result is given by

$$H = H_0 + H_{\rm int} \ , \tag{1}$$

where

$$H_0 = \sum_{m,n,a,b,\sigma} t_{ab}^{mn} a_{m\sigma}^{\dagger} b_{n\sigma} \tag{2}$$

and

$$H_{\rm int} = \frac{1}{2} \sum_{\sigma,\tau} \sum_{m,a,b,c,d} V_{abcd} a_{m\sigma}^{\dagger} c_{m\tau}^{\dagger} d_{m\tau} b_{m\sigma} \ . \tag{3}$$

The noninteracting part of the Hamiltonian, H_0, describes the itinerant electrons and, if necessary, it includes the crystal-field splitting for A_4C_{60} originated in the bct structure. We denote the transfer integrals between the orbital a at the molecule m and the orbital b at the molecule n by t_{ab}^{mn}, where a and b denote the t_{1u} orbitals, x, y, and z. We also denote the creation (annihilation) operator of the t_{1u} electron with the spin σ in the orbital a at the molecule m by $a_{m\sigma}^{\dagger}$ ($a_{m\sigma}$). The coupling constants of the effective electron-electron interaction, V_{abcd}, are classified into the intraorbital repulsion, $V_{\rm intra}$, the interorbital repulsion, $V_{\rm inter}$, the exchange interaction, J, and the pair transfer interaction, K. These coupling constants are given as follows:

$$V_{\rm intra} = V_{xxxx} = U_{xxxx} - \frac{1}{2} S_{Ag} - \frac{1}{2} S_{Hg} \ , \tag{4}$$

$$V_{\rm inter} = V_{xxyy} = U_{xxyy} - \frac{1}{2} S_{Ag} + \frac{1}{4} S_{Hg} \ , \tag{5}$$

$$J = V_{xyyx} = U_{xyyx} - \frac{3}{8} S_{Hg} \ , \tag{6}$$

and

$$K = V_{xyxy} = U_{xyxy} - \frac{3}{8} S_{Hg} \ . \tag{7}$$

Here, U_{xxxx} and U_{xxyy} are the intraorbital and interorbital repulsions originated in the screened Coulomb interaction, respectively. Furthermore, U_{xyyx} and U_{xyxy} are the exchange and pair transfer interactions also originated in the screened Coulomb interaction, respectively. The effects of the electron-phonon interaction are also included in the above coupling constants; S_{Ag} and S_{Hg} are the coupling constants of the t_{1u} electrons to the A_g and H_g intramolecular phonons, respectively. In our model, the coupling constant of the pair transfer interaction K is the same as the coupling constant of the exchange interaction J. Also, it is worthwhile to notice that these coupling constants satisfy the relation from the symmetry, $V_{\rm intra} = V_{\rm inter} + 2K$. Consequently, we can take $V_{\rm intra}$ and K as two independent parameters. It should also be noted that these coupling constants are strongly affected by the electron-

phonon interaction; the intraorbital repulsion is reduced considerably while the interorbital repulsion is not and the exchange and pair transfer interactions, which are originally positive, become negative due to the coupling of the t_{1u} electrons to the intramolecular H_g phonons.

To perform the TDA calculations, it is necessary to obtain the Hartree-Fock ground state, $|\mathrm{G}\rangle$, because the excitations are created over $|\mathrm{G}\rangle$ and the excited states are represented by the linear combination of such excitations as explained in the next section. The detailed procedure of the Hartree-Fock calculations is found elsewhere.[14] We rewrite the Hamiltonian H as follows:

$$H = H_{\mathrm{HF}} + \Delta H \ , \tag{8}$$

where

$$H_{\mathrm{HF}} = \sum_{\alpha \boldsymbol{k}\sigma} \varepsilon_{\alpha}^{\boldsymbol{k}} \alpha_{\boldsymbol{k}\sigma}^{\dagger} \alpha_{\boldsymbol{k}\sigma} \tag{9}$$

and

$$\Delta H = H - H_{\mathrm{HF}} \ . \tag{10}$$

The band energies for the itinerant electrons above are denoted by $\varepsilon_{\alpha}^{\boldsymbol{k}}$ and the corresponding creation (annihilation) operators by $\alpha_{\boldsymbol{k}\sigma}^{\dagger}$ ($\alpha_{\boldsymbol{k}\sigma}$), where α (α=ξ, η, and ζ) is the band index and $\boldsymbol{k}$ is the wave vector. The band indices used in the present study are labeled in such order that $\varepsilon_{\xi}^{\boldsymbol{k}} < \varepsilon_{\eta}^{\boldsymbol{k}} < \varepsilon_{\zeta}^{\boldsymbol{k}}$ at a given wave vector $\boldsymbol{k}$. For A_4C_{60}, ξ and η denote the occupied t_{1u} bands while ζ denotes the unoccupied t_{1u} band. We take the origin of the band energies at the top of the occupied t_{1u} bands throughout.

By using the eigenfunctions obtained by the Hartree-Fock calculations, we here define the coupling constants $V_{\alpha\beta\gamma\delta}^{\boldsymbol{k}_1\boldsymbol{k}_2\boldsymbol{k}_3\boldsymbol{k}_4}$ as follows:

$$V_{\alpha\beta\gamma\delta}^{\boldsymbol{k}_1\boldsymbol{k}_2\boldsymbol{k}_3\boldsymbol{k}_4} = \sum_{m,a,b,c,d} V_{abcd} \langle \alpha \boldsymbol{k}_1 | am \rangle \langle \gamma \boldsymbol{k}_3 | cm \rangle \langle dm | \delta \boldsymbol{k}_4 \rangle \langle bm | \beta \boldsymbol{k}_2 \rangle \ , \tag{11}$$

where $|am\rangle$ represents the electron in the orbital a at the molecule m and $|\alpha\boldsymbol{k}\rangle$ represents the eigenfunction corresponding to the eigenvalue $\varepsilon_{\alpha}^{\boldsymbol{k}}$; for simplicity, we leave out the spin index in the above.

We now give the order of magnitude of the coupling constants introduced here. First, U_{xxxx} and U_{xxyy} are of the order of about 0.6 eV while U_{xyxy} and U_{xyyx} are of the order of about 0.03 eV. This estimation is based on the calculations using the molecular orbitals obtained from the Hartree-Fock calculations.[14] Next, S_{Ag} and S_{Hg} are of the order of about 0.4 eV; we estimate this from the results of the Hartree-Fock study on the Jahn-Teller effect in the C_{60}^{-} anion.[17] Accordingly, V_{intra} and K are estimated to be about 0.2 eV and -0.1 eV, respectively, and also V_{inter} to be about 0.4 eV. In the present study, we use $V_{\mathrm{intra}} = 0.26$ eV and $K = -0.16$ eV, which are determined so as to reproduce the critical temperature of

superconductivity and the energy of the satellite in the photoemission spectra of K_3C_{60}.[16)]

3. TDA

We first introduce four types of operators that create excitations over the ground state $|\mathrm{G}\rangle$ obtained by the Hartree-Fock calculations. One is for the spin-singlet excitations:

$$\alpha^{\mathrm{S}}_{\boldsymbol{qk}} = \frac{1}{\sqrt{2}}(\zeta^{\dagger}_{\boldsymbol{k}+\boldsymbol{q}\uparrow}\alpha_{\boldsymbol{k}\uparrow} + \zeta^{\dagger}_{\boldsymbol{k}+\boldsymbol{q}\downarrow}\alpha_{\boldsymbol{k}\downarrow}) \ . \tag{12}$$

The other three are for the spin-triplet excitations:

$$\alpha^{\mathrm{T}+}_{\boldsymbol{qk}} = \zeta^{\dagger}_{\boldsymbol{k}+\boldsymbol{q}\uparrow}\alpha_{\boldsymbol{k}\downarrow} \ , \tag{13}$$

$$\alpha^{\mathrm{T}0}_{\boldsymbol{qk}} = \frac{1}{\sqrt{2}}(\zeta^{\dagger}_{\boldsymbol{k}+\boldsymbol{q}\uparrow}\alpha_{\boldsymbol{k}\uparrow} - \zeta^{\dagger}_{\boldsymbol{k}+\boldsymbol{q}\downarrow}\alpha_{\boldsymbol{k}\downarrow}) \ , \tag{14}$$

and

$$\alpha^{\mathrm{T}-}_{\boldsymbol{qk}} = \zeta^{\dagger}_{\boldsymbol{k}+\boldsymbol{q}\downarrow}\alpha_{\boldsymbol{k}\uparrow} \ . \tag{15}$$

In the above expressions, α represents the occupied bands, ξ and η. These operators create an electron in the ζ band, which is the unoccupied one, and a hole in the α band, which is one of the occupied bands. The Schrödinger equation that the excited states follow is

$$H\sum_{\alpha\boldsymbol{k}} f^{\alpha X}_{\boldsymbol{qk}}\alpha^{X}_{\boldsymbol{qk}}|\mathrm{G}\rangle = (E_{\mathrm{G}} + \hbar\omega_{\boldsymbol{q}})\sum_{\alpha\boldsymbol{k}} f^{\alpha X}_{\boldsymbol{qk}}\alpha^{X}_{\boldsymbol{qk}}|\mathrm{G}\rangle \ , \tag{16}$$

where X is S, T+, T0, or T$-$, $f^{\alpha X}_{\boldsymbol{qk}}$ is the expansion coefficient, E_{G} is the energy of the ground state, and $\hbar\omega_{\boldsymbol{q}}$ is the excitation energy. By using the relation

$$H\alpha^{X}_{\boldsymbol{qk}} = \left[H, \alpha^{X}_{\boldsymbol{qk}}\right] + \alpha^{X}_{\boldsymbol{qk}}H \tag{17}$$

in the left-side hand of eq.(16), we obtain

$$\sum_{\alpha\boldsymbol{k}} f^{\alpha X}_{\boldsymbol{qk}}\left\{\left[H, \alpha^{X}_{\boldsymbol{qk}}\right] - \hbar\omega_{\boldsymbol{q}}\alpha^{X}_{\boldsymbol{qk}}\right\}|\mathrm{G}\rangle = 0 \ . \tag{18}$$

We now write down explicit expressions of the above equations. Let us first consider the operator that create a spin-singlet excitation:

$$\xi^{\mathrm{S}}_{\boldsymbol{qk}} = \frac{1}{\sqrt{2}}(\zeta^{\dagger}_{\boldsymbol{k}+\boldsymbol{q}\uparrow}\xi_{\boldsymbol{k}\uparrow} + \zeta^{\dagger}_{\boldsymbol{k}+\boldsymbol{q}\downarrow}\xi_{\boldsymbol{k}\downarrow}) \tag{19}$$

and

$$\eta^{\mathrm{S}}_{\boldsymbol{qk}} = \frac{1}{\sqrt{2}}(\zeta^{\dagger}_{\boldsymbol{k}+\boldsymbol{q}\uparrow}\eta_{\boldsymbol{k}\uparrow} + \zeta^{\dagger}_{\boldsymbol{k}+\boldsymbol{q}\downarrow}\eta_{\boldsymbol{k}\downarrow}) \ . \tag{20}$$

Within TDA, we obtain the following eigenvalue equation:

$$\sum_{\boldsymbol{k}}\Bigg\{-\sum_{\boldsymbol{k}'}V^{\boldsymbol{k}'+\boldsymbol{q}\boldsymbol{k}+\boldsymbol{q}\boldsymbol{k}\boldsymbol{k}'}_{\zeta\zeta\xi\xi}\xi^{\rm S}_{\boldsymbol{q}\boldsymbol{k}'}f^{\xi{\rm S}}_{\boldsymbol{q}\boldsymbol{k}'}+2\sum_{\boldsymbol{k}'}V^{\boldsymbol{k}'+\boldsymbol{q}\boldsymbol{k}'\boldsymbol{k}\boldsymbol{k}+\boldsymbol{q}}_{\zeta\xi\xi\zeta}\xi^{\rm S}_{\boldsymbol{q}\boldsymbol{k}'}f^{\xi{\rm S}}_{\boldsymbol{q}\boldsymbol{k}'}$$
$$-\sum_{\boldsymbol{k}'}V^{\boldsymbol{k}'+\boldsymbol{q}\boldsymbol{k}+\boldsymbol{q}\boldsymbol{k}\boldsymbol{k}'}_{\zeta\zeta\xi\eta}\eta^{\rm S}_{\boldsymbol{q}\boldsymbol{k}'}f^{\eta{\rm S}}_{\boldsymbol{q}\boldsymbol{k}'}+2\sum_{\boldsymbol{k}'}V^{\boldsymbol{k}'+\boldsymbol{q}\boldsymbol{k}'\boldsymbol{k}\boldsymbol{k}+\boldsymbol{q}}_{\zeta\eta\xi\zeta}\eta^{\rm S}_{\boldsymbol{q}\boldsymbol{k}'}f^{\eta{\rm S}}_{\boldsymbol{q}\boldsymbol{k}'} \tag{21}$$
$$+(\varepsilon^{\boldsymbol{k}+\boldsymbol{q}}_{\zeta}-\varepsilon^{\boldsymbol{k}}_{\xi})\xi^{\rm S}_{\boldsymbol{q}\boldsymbol{k}}f^{\xi{\rm S}}_{\boldsymbol{q}\boldsymbol{k}}-\hbar\omega_{\boldsymbol{q}}\xi^{\rm S}_{\boldsymbol{q}\boldsymbol{k}}f^{\xi{\rm S}}_{\boldsymbol{q}\boldsymbol{k}}\Bigg\}|{\rm G}\rangle=0$$

and

$$\sum_{\boldsymbol{k}}\Bigg\{-\sum_{\boldsymbol{k}'}V^{\boldsymbol{k}'+\boldsymbol{q}\boldsymbol{k}+\boldsymbol{q}\boldsymbol{k}\boldsymbol{k}'}_{\zeta\zeta\eta\eta}\eta^{\rm S}_{\boldsymbol{q}\boldsymbol{k}'}f^{\eta{\rm S}}_{\boldsymbol{q}\boldsymbol{k}'}+2\sum_{\boldsymbol{k}'}V^{\boldsymbol{k}'+\boldsymbol{q}\boldsymbol{k}'\boldsymbol{k}\boldsymbol{k}+\boldsymbol{q}}_{\zeta\eta\eta\zeta}\eta^{\rm S}_{\boldsymbol{q}\boldsymbol{k}'}f^{\eta{\rm S}}_{\boldsymbol{q}\boldsymbol{k}'}$$
$$-\sum_{\boldsymbol{k}'}V^{\boldsymbol{k}'+\boldsymbol{q}\boldsymbol{k}+\boldsymbol{q}\boldsymbol{k}\boldsymbol{k}'}_{\zeta\zeta\eta\xi}\xi^{\rm S}_{\boldsymbol{q}\boldsymbol{k}'}f^{\xi{\rm S}}_{\boldsymbol{q}\boldsymbol{k}'}+2\sum_{\boldsymbol{k}'}V^{\boldsymbol{k}'+\boldsymbol{q}\boldsymbol{k}'\boldsymbol{k}\boldsymbol{k}+\boldsymbol{q}}_{\zeta\xi\eta\zeta}\xi^{\rm S}_{\boldsymbol{q}\boldsymbol{k}'}f^{\xi{\rm S}}_{\boldsymbol{q}\boldsymbol{k}'} \tag{22}$$
$$+(\varepsilon^{\boldsymbol{k}+\boldsymbol{q}}_{\zeta}-\varepsilon^{\boldsymbol{k}}_{\eta})\eta^{\rm S}_{\boldsymbol{q}\boldsymbol{k}}f^{\eta{\rm S}}_{\boldsymbol{q}\boldsymbol{k}}-\hbar\omega_{\boldsymbol{q}}\eta^{\rm S}_{\boldsymbol{q}\boldsymbol{k}}f^{\eta{\rm S}}_{\boldsymbol{q}\boldsymbol{k}}\Bigg\}|{\rm G}\rangle=0\ .$$

We next write down the Schrödinger equation for spin-triplet excitations. It is sufficient to consider the following two operators:

$$\xi^{\rm T+}_{\boldsymbol{q}\boldsymbol{k}}=\zeta^{\dagger}_{\boldsymbol{k}+\boldsymbol{q}\uparrow}\xi_{\boldsymbol{k}\downarrow} \tag{23}$$

and

$$\eta^{\rm T+}_{\boldsymbol{q}\boldsymbol{k}}=\zeta^{\dagger}_{\boldsymbol{k}+\boldsymbol{q}\uparrow}\eta_{\boldsymbol{k}\downarrow}\ . \tag{24}$$

We obtain the following eigenvalue equation:

$$\sum_{\boldsymbol{k}}\Bigg\{-\sum_{\boldsymbol{k}'}V^{\boldsymbol{k}'+\boldsymbol{q}\boldsymbol{k}+\boldsymbol{q}\boldsymbol{k}\boldsymbol{k}'}_{\zeta\zeta\xi\xi}\xi^{\rm T+}_{\boldsymbol{q}\boldsymbol{k}'}f^{\xi{\rm T+}}_{\boldsymbol{q}\boldsymbol{k}'}-\sum_{\boldsymbol{k}'}V^{\boldsymbol{k}'+\boldsymbol{q}\boldsymbol{k}+\boldsymbol{q}\boldsymbol{k}\boldsymbol{k}'}_{\zeta\zeta\xi\eta}\eta^{\rm T+}_{\boldsymbol{q}\boldsymbol{k}'}f^{\eta{\rm T+}}_{\boldsymbol{q}\boldsymbol{k}'}$$
$$+(\varepsilon^{\boldsymbol{k}+\boldsymbol{q}}_{\zeta}-\varepsilon^{\boldsymbol{k}}_{\xi})\xi^{\rm T+}_{\boldsymbol{q}\boldsymbol{k}}f^{\xi{\rm T+}}_{\boldsymbol{q}\boldsymbol{k}}-\hbar\omega_{\boldsymbol{q}}\xi^{\rm T+}_{\boldsymbol{q}\boldsymbol{k}}f^{\xi{\rm T+}}_{\boldsymbol{q}\boldsymbol{k}}\Bigg\}|{\rm G}\rangle=0 \tag{25}$$

and

$$\sum_{\boldsymbol{k}}\Bigg\{-\sum_{\boldsymbol{k}'}V^{\boldsymbol{k}'+\boldsymbol{q}\boldsymbol{k}+\boldsymbol{q}\boldsymbol{k}\boldsymbol{k}'}_{\zeta\zeta\eta\eta}\eta^{\rm T+}_{\boldsymbol{q}\boldsymbol{k}'}f^{\eta{\rm T+}}_{\boldsymbol{q}\boldsymbol{k}'}-\sum_{\boldsymbol{k}'}V^{\boldsymbol{k}'+\boldsymbol{q}\boldsymbol{k}+\boldsymbol{q}\boldsymbol{k}\boldsymbol{k}'}_{\zeta\zeta\eta\xi}\xi^{\rm T+}_{\boldsymbol{q}\boldsymbol{k}'}f^{\xi{\rm T+}}_{\boldsymbol{q}\boldsymbol{k}'}$$
$$+(\varepsilon^{\boldsymbol{k}+\boldsymbol{q}}_{\zeta}-\varepsilon^{\boldsymbol{k}}_{\eta})\eta^{\rm T+}_{\boldsymbol{q}\boldsymbol{k}}f^{\eta{\rm T+}}_{\boldsymbol{q}\boldsymbol{k}}-\hbar\omega_{\boldsymbol{q}}\eta^{\rm T+}_{\boldsymbol{q}\boldsymbol{k}}f^{\eta{\rm T+}}_{\boldsymbol{q}\boldsymbol{k}}\Bigg\}|{\rm G}\rangle=0\ . \tag{26}$$

In solving the above eigenvalue equations, we use 2000 $\boldsymbol{k}$ points and thus diagonalize 4000×4000 matrix for each case.

4. Results and Discussion

First of all, we show the results of the Hartree-Fock calculations carried out to obtain the ground state of A_4C_{60}. As mentioned in the previous section, the Hartree-Fock ground state

is the starting point in the TDA calculations because excitations are created over this ground state by applying the operators for creating excitations. The electronic structure and the density of states of A_4C_{60} obtained are shown in Figs. 1(a) and 1(b), respectively. The origin of energy is taken at the top of the occupied t_{1u} bands. It is found that the energy gap is about 0.8 eV. The gap consists of three contributions. To understand the origin of the energy gap, we first estimate the energy difference between the centers of the occupied and unoccupied t_{1u} bands. There are also three contributions in this difference. One is from the electron-electron interaction and is about 0.6 eV. The second is from the electron-phonon interaction and is about 0.4 eV. The third is from the crystal-field splitting and is about 0.2 eV. We thus find that the energy difference between the centers of the occupied and unoccupied t_{1u} bands is about 1.2 eV. The energy gap is finally estimated to be about 0.8 eV by considering the band width of about 0.4 eV. It should be noted that the most dominant contribution is from the electron-electron interaction and the next is from the electron-phonon interaction. It is also important to note that, if we consider only the crystal-field splitting, the insulating nature of A_4C_{60} cannot be explained. This is the reason why A_4C_{60} is called the Mott-Jahn-Teller insulator.[12)]

We next show the results of the TDA calculations for the excitation spectrum. The dispersion relation of excitations calculated by eqs.(21) and (22) and eqs.(25) and (26) is shown in Fig. 2. The lowest excitations around 0.3 eV, which consist of a pair of branches, correspond to the creation of the spin-singlet Frenkel excitons. The next lowest excitations around 0.6 eV, which also consist of a pair of branches, correspond to the creation of the spin-triplet Frenkel excitons. This result is in strong contrast to the excitons in usual insulators where the the creation energy of the spin-singlet Frenkel exciton is larger than that of the spin-triplet Frenkel exciton. The reason why the spin-singlet Frenkel exciton is energetically lower than the spin-triplet Frenkel exciton in A_4C_{60} is that the exchange interaction J is negative because the contribution from the electron-phonon interaction overcomes the Hund coupling originated in the Coulomb repulsion.[14,15)] Furthermore, excitations which exist over 0.8 eV correspond to the creation of a pair of a free electron and a free hole; the free electron is created in the upper t_{1u} band and the free hole is created in the lower t_{1u} bands. This type of excitations are very similar to the Stoner excitation in the Mott-Hubbard insulators and form a continuous spectrum as shown in Fig. 2.

The reason for the existence of the two branches of each exciton band is that, since the upper t_{1u} band is single and unoccupied and the lower t_{1u} bands are double and occupied, there arise two branches of Frenkel excitons; this is very similar to the Davidov splitting, which occurs in a system where two kind of excitations exist in the unit cell. A typical system for the Davidov splitting is the benzene crystal whose unit cell consists of a pair of benzene molecules; the excitations of the two benzene molecules couple to form one bonding-type exciton and

one antibonding-type exciton. In A_4C_{60}, the two lower t_{1u} levels play a similar role to the excitation of the two benzene molecules.

In the present study, we restrict ourselves within the model which takes account of only the intramolecular Coulomb repulsion between the t_{1u} electrons. It may, however, be more realistic to take account of the nearest-neighbor intermolecular Coulomb repulsion between the t_{1u} electrons as well; this can result in the formation of the charge transfer excitons. The order of magnitude of the nearest-neighbor intermolecular Coulomb repulsion can be estimated by considering the ratio between the average distance between two t_{1u} electrons in a single C_{60} molecule, which is about 4 Å, and the average distance between two t_{1u} electrons in a nearest-neighbor pair of C_{60} molecules, which is about 11 Å. Since the order of magnitude of the intramolecular Coulomb repulsion is about 0.6 eV, the order of magnitude of the nearest-neighbor intermolecular Coulomb repulsion is estimated to be about 0.2 eV. As a result, the charge transfer excitons can appear at about 1 eV, i.e., at the energy lower by about 0.2 eV with respect to the center of the continuous spectrum in Fig. 2. We thus believe that the present results obtained for the Frenkel excitons are almost unchanged if the nearest-neighbor intermolecular Coulomb repulsion is taken into account.

We finally compare the present results with experimental results available for the excited states of A_4C_{60}. Several experimental studies on the excited states of A_4C_{60} has been carried out so far. One is the result of the infrared reflection measurement.[10] Another is the result of the measurement of the electron-energy-loss spectrum (EELS).[11] Since the creation process of the Frenkel excitons studied here, i.e., the intramolecular $t_{1u} \rightarrow t_{1u}$ transition, is optically forbidden, we compare the present results with the EELS results. In the EELS spectra, two features are clearly seen in that of Rb_4C_{60}. One is at about 0.3 eV and the other is at about 0.6 eV; although the two features in the EELS spectra of K_4C_{60} and Cs_4C_{60} is not so clear than those in Rb_4C_{60}, such features possibly exist in the experimental spectra. We believe that the one at 0.3 eV is originated in the creation of the spin-singlet Frenkel excitons and the other at 0.6 eV is originated in the creation of the spin-triplet Frenkel excitons. Although the EELS spectra for K_4C_{60}, Rb_4C_{60}, and Cs_4C_{60} are quite similar to each other, the spectrum for Na_4C_{60} are largely different from those for K_4C_{60}, Rb_4C_{60}, and Cs_4C_{60}. At present, the origin of the discrepancy is not clear. One possible reason for the discrepancy is that the crystal structure of Na_4C_{60} is different from the structure of K_4C_{60}, Rb_4C_{60}, and Cs_4C_{60}; the structure of Na_4C_{60} is fcc while the structure of the other three materials is bct.[11,18,19] It is, however, necessary for elucidating the origin of this discrepancy to study Na_4C_{60} in detail both experimentally and theoretically in the future.

5. Summary

We have studied low-energy excitations in A_4C_{60} by using the Tamm-Dancoff approximation. It is found that the lowest excitation corresponds to the creation of the spin-singlet

Frenkel excitons at about 0.3 eV and the next lowest excitation corresponds to the creation of the spin-triplet Frenkel excitons at about 0.6 eV. This result is in strong contrast to usual insulators where the creation energy of the spin-singlet exciton is larger than that of the spin-triplet exciton.

Acknowledgements

We would like to thank Y. Iwasa for valuable discussions. The numerical calculations were carried out on Fujitsu VPP5000 of Science Information Processing Center, University of Tsukuba.

References

1) *Solid State Physics*, Vol. 48, eds. H. Ehrenreich and F. Spaepen (Academic Press, New York, 1994).
2) A. F. Hebard, M. J. Rosseinsky, R. C. Haddon, D. W. Murphy, S. H. Glarum, T. T. M. Palstra, A. P. Ramirez, and A. R. Kortan: Nature **350** (1991) 600.
3) M. J. Rosseinsky, A. P. Ramirez, S. H. Glarum, D. W. Murphy, R. C. Haddon, A. F. Hebard, T. T. M. Palstra, A. R. Kortan, S. M. Zahurak, and A. V. Makhija: Phys. Rev. Lett. **66** (1991) 2830.
4) K. Tanigaki, T. W. Ebbesen, S. Saito, J. Mizuki, J. S. Tsai, Y. Kubo, and S. Kuroshima: Nature **352** (1991) 222.
5) H. Kitano, R. Matsuo, K. Miwa, A. Maeda, T. Takenobu, Y. Iwasa, and T. Mitani: Phys. Rev. Lett. **88** (2002) 096401.
6) R. Tycko, G. Dabbagh, M. J. Rosseinsky, D. W. Murphy, A. P. Ramirez, and R. M. Fleming: Phys. Rev. Lett. **68** (1992) 1912.
7) R. F. Kiefl, T. L. Duty, J. W. Schneider, A. MacFarlane, K. Chow, J. W. Elzey, P. Mendels, G. D. Morris, J. H. Brewer, E. J. Ansaldo, C. Niedermayer, D. R. Noakes, C. E. Stronach, B. Hitti, and J. E. Fischer: Phys. Rev. Lett. **69** (1992) 2005.
8) M. Kosaka, K. Tanigaki, I. Hirosawa, Y. Shimakawa, S. Kuroshima, T. W. Ebbesen, J. Mizuki, and Y. Kubo: Chem. Phys. Lett. **203** (1993) 429.
9) I. Lukyanchuk, N. Kirova, F. Rachdi, C. Goze, P. Molinie, and M. Mehring: Phys. Rev. B **51** (1995) 3978.
10) Y. Iwasa and T. Kaneyasu: Phys. Rev. B **51** (1995) 3678.
11) M. Knupfer and J. Fink: Phys. Rev. Lett. **79** (1997) 2714. ¡¡ Mott-Jahn-Teller Insulator A4C60 ¿¿
12) M. Fabrizio and E. Tosatti: Phys. Rev. B **55** (1997) 13465.
13) O. Gunnarson: Rev. Mod. Phy. **69** (1997) 575.
14) S. Suzuki and K. Nakao: Phys. Rev. B **52** (1995) 14206.
15) S. Suzuki, S. Okada, and K. Nakao: J. Phys. Soc. Jpn. **69** (2000) 2615.
16) T. Chida, S. Suzuki, and K. Nakao: J. Phys. Soc. Jpn. **71** (2002) 525.
17) N. Koga and K. Morokuma: Chem. Phys. Lett. **196** (1992) 191.
18) D. W. Murphy, M. J. Rosseinsky, R. M. Fleming, R. Tycko, A. P. Ramirez, R. C. Haddon, T. Siegrist, G. Dabbagh, J. C. Tully, and R. E. Walstedt: J. Phys. Chem. Solids **53** (1992) 1321.
19) M. J. Rosseinsky, D. W. Murphy, R. M. Fleming, R. Tycko, A. P. Ramirez, G. Dabbagh, and S. E. Barrett: Nature **356** (1992) 416.

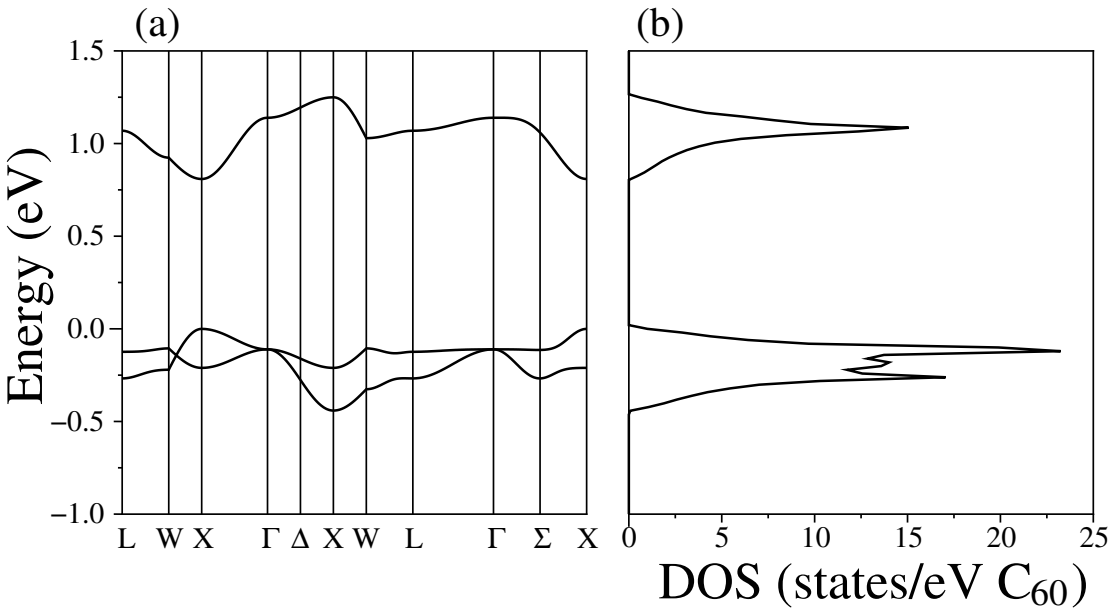

Fig. 1. (a)Band structure and (b)density of states of A_4C_{60} obtained by the Hartree-Fock calculations. The origin of energy is taken at the top of the occupied t_{1u} bands.

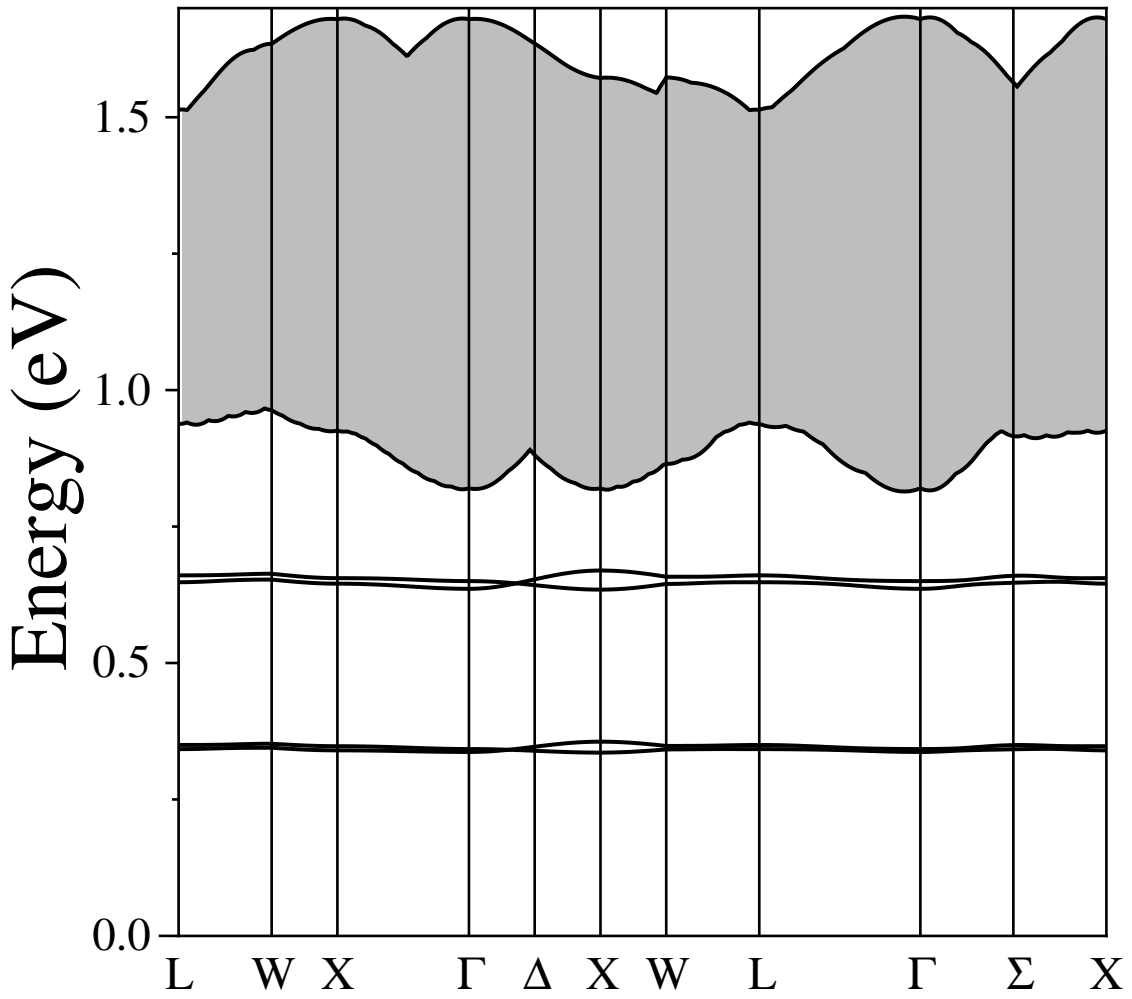

Fig. 2. Dispersion relation of excitations in A_4C_{60}. The lowest branches at about 0.3 eV are of the spin-singlet excitons and the next branches at about 0.6 eV are of the spin-triplet excitons. The hatched region represents the excitation of a pair of a free electron and a free hole, which form a continuous spectrum.